where ΔZPE is the difference in zero-point energies between AHA^- (AH) and ADA^- (AD). The value for ΔZPE was determined as one-half the sum of the vibrational frequencies for each species except as described below. For CH_3OH and CH_3OD, the calculated value for ΔZPE is 746 cm^{-1} as compared to an experimental value of 681 cm^{-1}.[34] (This latter value is not precise as the torsional frequency is not well-determined experimentally.) For the proton-bound dimers the situation is complicated by the fact that the asymmetric stretch of the proton (deuteron) is not well-treated in the harmonic approximation. We thus define the ZPE to be one-half the sum of all of the modes excluding the asymmetric stretch. We take the value for the asymmetric stretch zero-point frequency from that determined for the model potential V_3. The value for ΔZPE for the asymmetric stretch is 130 cm^{-1}. (Examination of Kreevoy's other potentials[7] shows that ΔZPE is not strongly dependent on the barrier height and even with no barrier has a value of 200 cm^{-1}.) The asymmetric stretch in the proton-bound dimer is quite distinct. Although this mode can be found in the deuteron-bound dimer, there is also a slightly higher lying mode with some asymmetric stretch character. From the above results, the calculated ΔZPE for the dimer is 530 cm^{-1}. Substitution into eq 16 gives a calculated value for K_6 of 0.35, in excellent agreement with the observed value of 0.31, especially considering the approximations made in determining ΔZPE and in the use of eq 16. The use of eq 16 assumes that the ratio of the translational, rotational, and electronic partition functions is unity. This should be a good approximation since there should not be large isotope effects on these quantities. Another approximation in eq 16 is that the temperature dependences of the vibrational populations were neglected. Examination of the vibrations for the dimers shows that this is not that severe an approximation for $AH(D)A^-$ since the lowest lying modes (those that would be thermally populated) do not exhibit a large isotope dependence. This is not surprising since the vibrational modes involving the proton (deuteron) are at higher frequencies. There is likely to be a larger contribution from the monomer since the torsional potential does exhibit some isotope effect.

The good agreement of the calculated value of K_6 with the experimental value is consistent with Kreevoy's discussion[7] of the role of the bending modes in raising the value of ϕ from that predicted by using only the asymmetric stretch. Although his discussion was qualitative, our results demonstrate that the modes external to the asymmetric stretch will indeed raise the value ϕ and thus moderate the isotope effect. However, the value for ϕ_{gp} is still far from unity and demonstrates the presence of a large isotope effect. Comparison with our previous work on $A = EtO^-$ shows that substitution of Et for Me raises ϕ_{gp} from 0.33 to 0.46. Whether this is due to a change in the central barrier height or to the presence of additional modes external to the asymmetric stretch cannot be determined at this time.

Registry No. Methoxide anion, 3315-60-4.

Reversible Formation and Disruption of Micelles by Control of the Redox State of the Head Group

T. Saji,* K. Hoshino, and S. Aoyagui

Contribution from the Department of Chemical Engineering, Tokyo Institute of Technology, Ohokayama, Meguro-ku, Tokyo 152, Japan. *Received January 3, 1985*

Abstract: Electrochemical and spectroscopic studies of a functional surfactant, (ferrocenylmethyl)dodecyldimethylammonium bromide (I^+) with ferrocene as the redox moiety, are reported. The concentration dependence of the diffusion coefficient values for I^+ and its oxidized form I^{2+} show that the I^+ surfactants form redox-active micelles and that these micelles can be broken up into monomers by oxidation and re-formed by reduction. Feasibility of such reversible control of the formation–disruption of micelles is also demonstrated by a spectroscopic observation that a dye is solubilized or released according as the micelles are formed or broken up. In addition, the result of potential-step chronoamperometry is interpreted on the basis of the Nernst diffusion-layer model.

Functional micelles, i.e., aggregates of surfactant molecules to which functional groups are covalently bonded, possess advantages over nonfunctional ones in the following aspects: (1) ability to undergo specific reactions, e.g., redox reactions,[1,7] (2) effective charge separation by using the functional surfactant as an electron acceptor,[2-4] (3) reaction media in concentrating or fixing active sites,[5] and (4) probes for the microenvironment of micelles.[6] No studies have so far dealt with the effect of functional groups on the dynamic properties of micelles, e.g., the self-assembling behavior, or the static ones, e.g., the CMC and the aggregation number. The present paper deals with the reversible formation and disruption of micelles by control of the redox state of the surfactant-head group.[7] The electroactive surfactant studied is the bromide salt of $FcCH_2N^+(CH_3)_2C_{12}H_{25}$ (I^+), where Fc represents the ferrocene moiety.

Experimental Section

The bromide salt of I^+ was prepared by the following procedures: The mixture of equimolar amounts of ((dimethylamino)methyl)ferrocene (Aldrich) and *n*-dodecyl bromide (Tokyo Kasei) was stirred for 2 h at 60 °C. The reaction product was recrystallized twice from acetone to give a yellow, crystalline product in 63% yield. It was identified by the elemental analysis. Calcd for $C_{25}H_{42}NFeBr$: C, 60.9; H, 8.6; N, 2.7. Found: C, 60.8; H, 8.6; N, 2.7. The IR and the electronic spectra for I^+ were respectively in fair agreement with those for ferrocene.[8] Li_2SO_4

(1) Takuma, K.; Sakamoto, T.; Nagamura, T.; Matsuo, T. *J. Phys. Chem.* **1981**, *85*, 619.
(2) Brugger, P. A.; Grätzel, M. *J. Am. Chem. Soc.* **1980**, *102*, 2461.
(3) Brugger, P. A.; Infelta, P. P.; Braun, A. M.; Grätzel, M. *J. Am. Chem. Soc.* **1981**, *103*, 320.
(4) Humphry-Barker, R.; Grätzel, M.; Tundo, P.; Plelizetti, E. *Angew. Chem., Int. Ed. Engl.* **1979**, *18*, 630.
(5) Fendler, J. H. "Membrane Mimetic Chemistry"; Wiley: New York, 1982; pp 339-409.
(6) Menger, F. M.; Chow, J. F. *J. Am. Chem. Soc.* **1983**, *105*, 5501.
(7) The preliminary study of the reversible formation and disruption of micelles by control of the redox state of the head group was reported: Saji, T.; Hoshino, K.; Aoyagui, S.; *J. Chem. soc., Chem. Commun.* **1985**, 865.

0002-7863/85/1507-6865$01.50/0

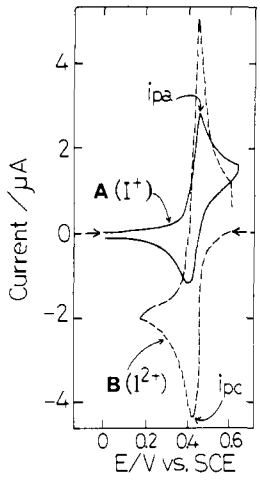

Figure 1. Cyclic voltammograms for solutions of (A) 2.0 mM of I^+ (—) and (B) 2.0 mM of I^{2+} prepared by bulk electrolysis (---) in 0.2 M Li_2SO_4 at 25 °C. Scan rate: 20 mV s^{-1}. Working electrode area: 0.021 cm^2.

(Wako Pure Chemicals, reagent grade), $Ce(SO_4)_2$ (Wako Pure Chemicals, reagent grade), and hydroquinone (Wako Pure Chemicals, reagent grade) were commercially obtained and used as supplied.

Electrochemical and spectroscopic measurements were carried out at 25 °C under a nitrogen atmosphere, by using test solutions containing 0.2 M Li_2SO_4 as the supporting electrolyte. All solutions were prepared with doubly distilled water. Voltammetric behavior of I^+ was investigated by cyclic voltammetry with a three-electrode potentiostat equipped with circuitry for the compensation of solution resistance. A platinum disk electrode and a saturated calomel electrode (SCE) were used respectively as the working and the reference electrodes. An aqueous saturated Li_2SO_4 bridge was used to connect the I^+ solution in the electrolysis cell with the SCE, because I^+ precipitated upon contact with the KCl bridge of the SCE.

The apparent diffusion coefficients (D_{app}) of I^+ and I^{2+} was determined by potential-step chronoamperometry[9] in which a one-electron process was assumed.[10] The current–time curves were recorded on a Yokogawa TECHNICORDER X TYPE 3083 recorder equipped with a Riken Denshi Model TCC-1000-11 transient memory.

The micellar weight of I^+ was determined by the quasielastic light-scattering method[11] on a Chromatix KMX-6 Low Angle Scattering Photometer. The electronic spectra of the dye in I^+ and I^{2+} solutions were recorded on a Hitachi UV 220A spectrophotometer.

Results and Discussion

The cyclic voltammogram of 2.0 mM I^+ shows the reversible one-electron oxidation step with a half-wave potential ($E_{1/2}$) of +0.428 V vs. SCE with a scan rate 20 mV s^{-1} (Figure 1A). The value of $E_{1/2}$ was determined by using the relationship $E_{1/2} = E_{pc} + 29$ mV, because of the weak adsorption of I^+, where E_{pc} is the cathodic peak potential. The number of electrons (n) involved in the electrode process was determined by using the relationship $E_{pc} - E_{pc/2} = 56.5/n$ mV, where $E_{pc/2}$ is the cathodic half-peak potential.[10] The cyclic voltammogram of 2.0 mM I^{2+} shows a reversible one-electron reduction step with $E_{1/2}$ of +0.440 V (Figure 1B). The solution of I^{2+} was prepared from the solution of I^+ by controlled-potential bulk electrolysis or by chemical oxidation with $Ce(SO_4)_2$. The cyclic voltammograms of I^+ in an oxidation–reduction cycle of $I^+ \rightarrow I^{2+} \rightarrow I^+$ showed that the yield of I^+ was 100%. In the electronic spectrum for the blue solution of I^{2+}, the shape and the positions of peaks at 466 and 628 nm agreed with those for ferrocenium ion.[12] I^{2+} was not a foaming agent, while the I^+ solution caused foam when stirred or bubbled. A plot of a cathodic peak current, i_{pc}, vs. the square root of a sweep rate, $v^{1/2}$, for the I^{2+} solution is linear; hence I^{2+} is not adsorbed on the electrode surface. The i_{pc} value for the I^{2+} solution is much greater than the anodic one for the I^+ solution, i_{pa}, though this i_{pa} is enhanced by the adsorption of I^+. This finding suggests that the diffusion coefficient value of I^{2+} is much greater than that of I^+ because i_{pc} and i_{pa} are proportional to the square root of the diffusion coefficient of I^{2+} and I^+, respectively.[9] As the value of a diffusion coefficient (D) is nearly proportional to the inverse of the square root of a molecular weight (M), $D \propto M^{-0.55}$,[13] the weight of the diffusion species in the I^{2+} solution is much lower than that in the I^+ solution.

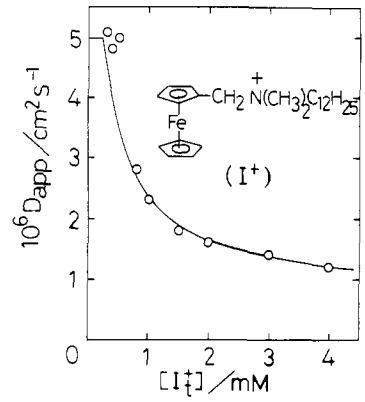

Figure 2. Plot of the apparent diffusion coefficient, D_{app}, vs. the total concentration of I^+, $[I_t^+]$. Circles: experimental points. Solid line: calculated from eq 6.

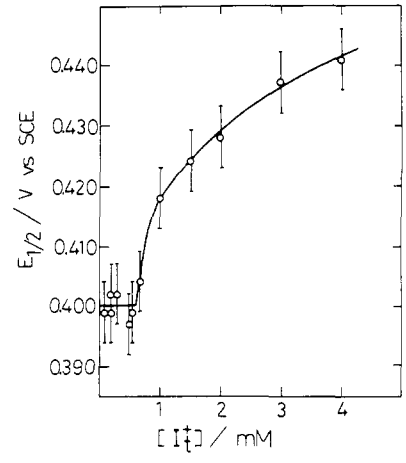

Figure 3. Plot of the half-wave potential, $E_{1/2}$, vs. the total concentration of I^+, $[I_t^+]$. Scan rate: 20 mV s^{-1}.

Figures 2 and 3 show the experimental plots of the apparent diffusion coefficient of I^+ (D_{app}) and $E_{1/2}$ vs. the total concentration of I^+ ($[I_t^+]$), respectively. A plot of the oxidation current for I^+ vs. $(\text{time})^{-1/2}$ deviates a straight line for times shorter than about 0.5 s after the potential step owing to the adsorption of I^+ on the electrode surface; however, for times ranging from 0.5 to 2.0 s the plot obeys the Cottrel equation.[9] Accordingly, the reactant adsorption is absent for times longer than 0.5 s. The D_{app} values were determined in 0.5–2.0 s. The abrupt changes in both values at 0.5 mM and the following gradual change with increasing $[I_t^+]$ may be attributed to a micelle formation at $[I_t^+] = 0.5$ mM. The CMC value of I^+ in 0.2 M Li_2SO_4 at 25 °C, 0.5 mM, was determined on this basis.[14] The reason for the abrupt decrease in D_{app} will be discussed later in some detail. The value of the diffusion coefficient of the I^+ monomer (D_m) was determined as

(8) Grasselli, J. G.; Ritchery, W. M. "Atras of Spectral Data and Physical Contents for Organic Compounds"; CRC Press, Inc.: Cleveland, Ohio, 1975; Vol. 3, p 311.
(9) Bard, A. J.; Faulkner, L. R. "ELECTROCHEMICAL METHODS"; Wiley: New York, 1980.
(10) Nicolson, R. S.; Shain, I. *Anal. Chem.* **1964**, *36*, 706.
(11) Shinoda, K.; Nakagawa, T.; Tamamushi, B.; Isemura, T. "Colloidal Surfactants"; Academic Press: New York and London, 1963; p 112.
(12) Traverso, O.; Scandola, F. *Inorg. Chim. Acta* **1970**, *4*, 493.
(13) E.g.: (a) Saji, T.; Nicholas, F. P.; Webber, S. E.; Bard, A. J.; *J. Phys. Chem.* **1978**, *82*, 1101. (b) Flanagan, J. B.; Margel, S.; Bard, A. J.; Anson, F. C. *J. Am. Chem. Soc.* **1978**, *100*, 4248. (c) Smith, T. W.; Kuder, J. E.; Wychick, D. *J. Polym. Sci.* **1976**, *14*, 2433.
(14) The solubility of I^+ in 0.2 M Li_2SO_4 aqueous solution at 25 ± 0.3 °C was 5.6 mM. Since the solution became turbid above this concentration, micelles might be formed in the concentration range of 0.5 to 5.6 mM.

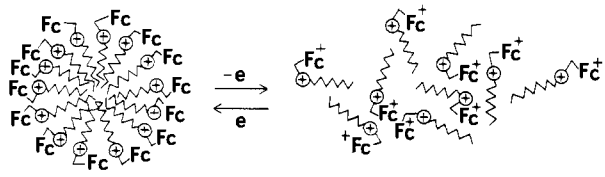

Figure 4. Schematic representation of reversible break-up and formation of I^+ micelles by redox reaction.

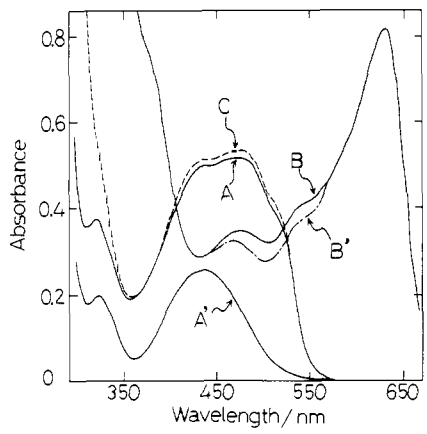

Figure 5. Electronic absorption spectra of TAN saturated in 0.2 M Li_2SO_4 containing (A) 2.0 mM I^+, (B) 2.0 mM I^{2+} generated by $Ce(SO_4)_2$ oxidation, and (C) 2.0 mM I^+ regenerated by hydroquinone reduction at 25 °C. A′ and B′ are the spectra for 2.0 mM I^+ and 2.0 mM I^{2+} not containing TAN, respectively.

$(5.0 \pm 0.5) \times 10^{-6}$ cm^2 s^{-1}, which is equal to the D_{app} value below the CMC.

The micellar weight of the I^+ micelles in 0.2 M Li_2SO_4 determined was 44600. The aggregation number (N) was determined as 91 ± 7. The influence of the micellar concentration on the light scattering was removed by the extrapolation to the value at CMC.[11]

On the other hand, the value of the diffusion coefficient of I^{2+} was kept unchanged at $(4.6 \pm 0.5) \times 10^{-6}$ cm^2 s^{-1} independently of $[I^{2+}]$. The fact that this value is nearly equal to the D_m value suggests that the I^{2+} molecules exist in the monomeric form, i.e., the micelles of I^+ may be broken up into the monomers by oxidation, probably owing to the enhancement in electrostatic repulsion among positively charged head groups and in their hydrophilic character as well (Figure 4).

The feasibility of control of micelle formation and disruption was also demonstrated by using a micelle-solubilized substance as a probe. The solubilizate used was 1-(*o*-tolylazo)naphthalen-2-ol (TAN) which was sparingly soluble in water and not oxidizable by $Ce(SO_4)_2$.

Figure 5 shows UV–vis absorption spectra of the following test solutions: solutions A, I^+ (2.0 mM) + TAN (saturated)[15] and A′, I^+ (2.0 mM); solutions B, I^{2+} (2.0 mM) + TAN (saturated) and B′, I^{2+} (2.0 mM); and solution C, I^+ (2.0 mM) + TAN (saturated) in 0.2 M Li_2SO_4 aqueous solution. Solution B was prepared by oxidation of solution A with $Ce(SO_4)_2$ and solution C by reduction of solution B with hydroquinone. It can be seen from Figure 5 that the amount of TAN in the I^{2+} solution, which can be estimated by subtracting the spectrum of solution B′ from that of solution B, is less than 10% relative to that of TAN solubilized in I^+ micelles, which can be estimated by subtracting the spectrum of A′ from that of A.

These findings suggest that the water-insoluble TAN is solubilized in the micelles of I^+, and, when I^+ is oxidized into I^{2+}, the micelles are broken up and TAN is released and precipitated. Furthermore, the reversibility of this process is demonstrated by the following experiment: addition of hydroquinone to solution B under stirring yielded the same spectrum as that of A (solution C, Figure 5C), which indicates the reformation of I^+ and hence its micelles and re-solubilization of TAN.

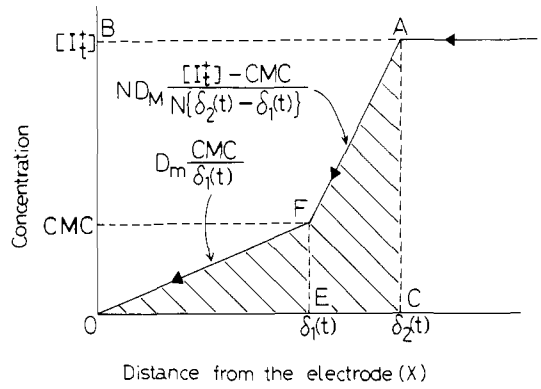

Figure 6. Concentration profile at an electrode for I^+; $x = 0$ corresponds to the electrode surface.

Model for the Electrode Reaction of I^+

We consider an experiment involving an instantaneous change in potential from a value where no electrolysis occurs to a value in the mass transfer-controlled region for oxidation of I^+ (potential-step chronoamperometry). One assumes the following diffusion layer model for I^+ (Figure 6) which is based on the Nernst diffusion-layer model:[9,16] Near the electrode surface exists an inner layer of thickness $\delta_1(t)$, in which only I^+ monomers exist and diffuse to the electrode surface along the concentration gradient of $CMC/\delta_1(t)$ where t is the time after the potential step; next to this layer exists an outer layer of thickness $(\delta_2(t) - \delta_1(t))$, in which the I^+ micelles break up so that the concentration of the I^+ monomers may be kept constant at CMC, so that only the micelles may diffuse toward the inner layer along the concentration gradient of $[I_M^+]/(\delta_2(t) - \delta_1(t))$ where $[I_M^+]$ is a micellar concentration equal to $([I_t^+] - CMC)/N$. Outside the second layer, convective transport maintains the concentration uniform at the bulk concentration $[I_t^+]$.

This model is based on the assumptions (1) that a micelle-formation equilibrium[17] is rapidly established through the whole electrode process, which makes it possible to keep the concentration of I^+ monomer at CMC in the region of EC and (2) that I^{2+} does not distort the concentration profile in Figure 6.

The flux of I^+ through the unit area of the surface C into the region OC owing to the growth of the second layer with time is given by

$$d([I_t^+]\delta_2(t))/dt$$

the flux of I^+ at the electrode is given by

$$D_m CMC/\delta_1(t)$$

on the other hand, the rate of increase of I^+ in the region OC is given by

$$d[CMC \cdot \delta_1(t)/2 + (CMC + [I_t^+])(\delta_2(t) - \delta_1(t))/2]dt$$

which is equal to the rate of increase of the zone AFOC (shaded part in Figure 6). Hence, we have immediately

$$d([I_t^+]\delta_2(t))/dt - D_m CMC/\delta_1(t) = d[CMC \cdot \delta_1(t)/2 + (CMC + [I_t^+])(\delta_2(t) - \delta_1(t))/2]/dt \quad (1)$$

At the surface E, the flux of the I^+ monomers in the OE region must be equal to that of the I^+ forming micelles in the region EC.

$$D_m \cdot CMC/\delta_1(t) = ND_M[I_M^+]/(\delta_2(t) - \delta_1(t)) \quad (2)$$

(15) Solution A was prepared as follows. A solution of 2.0 mM I^+ + 0.2 M Li_2SO_4 + an excess amount of TAN was deaerated by nitrogen bubbling, stirred vigorously, and then centrifuged at 25 °C. The supernatant solution was used in spectral measurements.

(16) Nernst, W. Z. *Phys. Chem.* **1904**, *47*, 52.

(17) Fendler, J. H.; Fendler, E. J. "Catalysis in Micellar and Macromolecular Systems"; Academic Press: New York, 1975; p 23.

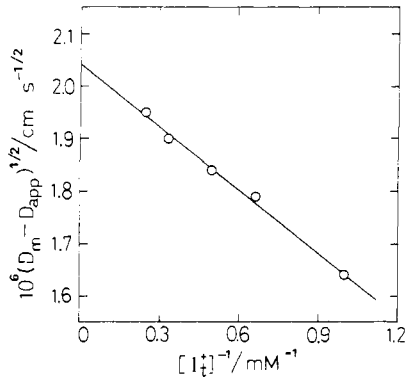

Figure 7. Plot of $(D_m - D_{app})^{1/2}$ vs. $[I_t^+]^{-1}$. The straight line is drawn by the least-squares method.

Substituting the solution $\delta_1(t)$ from eq 1 and 2 into the following expression for the current i

$$i = nFA[D_m \cdot CMC/\delta_1(t)] \quad (3)$$

where n is the number of electrons per molecule oxidized, F the faraday, and A the area of an electrode, we get

$$i = nFA[I_t^+]D_{app}^{1/2}/2t^{1/2} \quad (4)$$

where

$$D_{app} = (CMC/[I_t^+])(2 - CMC/[I_t^+])D_m + (1 - CMC/[I_t^+])^2 D_M \quad (5)$$

Equation 5 is rewritten as

$$(D_m - D_{app})^{1/2} = -CMC(D_m - D_M)^{1/2}[I_t^+]^{-1} + (D_m - D_M)^{1/2} \quad (6)$$

Figure 7 shows the plot of $(D_m - D_{app})^{1/2}$ vs. $[I_t^+]^{-1}$. The CMC and D_M values of 0.20 mM and 0.84 × 10^{-6} cm^2 s^{-1}, respectively, were determined from the slope and the intercept of the plot by using the foregoing D_m value of 5.0 × 10^{-6} cm^2 s^{-1}. The solid line in Figure 2 was drawn by using these values of D_M and CMC and the experimental value of D_m. A good linearity of the plot of Figure 7 and a satisfactory fitness of the calculated curve with experimental points in Figure 2 suggest that the electrode reaction of I^+ is reasonably explained by the model in Figure 6. There is a small difference in CMC between the experimental value (0.5 mM) and the calculated value (0.2 mM). It may come from the simplicity of the model used. Further details of this model are now under discussion.

Acknowledgment. The authors thank Professor S. Tazuke and Dr. T. Ikeda for use of the KMX-6 low-angle light-scattering photometer. They are grateful to Dr. M. Fujihira for his helpful discussion.

Registry No. I^+Br^-, 98778-40-6.

Dependence of Deuterium Spin–Lattice Relaxation Rates of Multilamellar Phospholipid Dispersions on Orientational Order[1]

Gerald D. Williams, James M. Beach, Steven W. Dodd, and Michael F. Brown*†

Contribution from the Department of Chemistry and Biophysics Program, University of Virginia, Charlottesville, Virginia 22901. *Received January 15, 1985*

Abstract: ^{2}H NMR studies of a homologous series of 1,2-diacyl-*sn*-glycero-3-phosphocholines with perdeuterated saturated chains, ranging in length from C12:0 to C16:0, have been performed with use of quadrupolar echo techniques at a resonance frequency of 55.4 MHz. Randomly oriented, multilamellar dispersions containing 50 wt % H_2O in the liquid crystalline (L_α) phase have been employed. The ^{2}H spin–lattice relaxation times (T_1) and C–^{2}H bond segmental order parameters (S_{CD}) of each of the resolved quadrupolar splittings have been obtained from the powder-type spectra, corresponding to a random distribution of orientations, as well as from the 0 °C oriented subspectra obtained by numerical deconvolution (de-Pakeing). Evidence that the spin–lattice relaxation rate profiles as a function of chain position $T_1^{-1}(i)$ are related to the corresponding order profiles $S_{CD}(i)$ by a square-law functional dependence has been obtained, indicative of a contribution from relatively slow fluctuations in the local bilayer ordering to the relaxation. The results suggest that two broad classes of motions influence the ^{2}H spin–lattice relaxation rates of lipid bilayers: rapid local motions, most likely due to bond rotational isomerizations and long-axis rotational diffusion of the lipid chains, as well as slower director fluctuations as found in other liquid crystalline mesophases.

I. Introduction

Deuterium (^{2}H) NMR has been widely utilized to investigate the molecular properties of lipid bilayers and biological membranes.[2-5] The ^{2}H nucleus has a spin $I = 1$, and the quadrupolar coupling with the electrostatic field gradient arising from its bonding environment is large relative to the magnetic dipolar interactions among ^{2}H and ^{1}H nuclei; thus a single interaction is dominant in most cases. While the relatively large size of the electric quadrupolar interaction introduces difficulties in obtaining ^{2}H NMR spectra, the interpretation of the results is correspondingly simplified.[2] Owing to the different time scales, ^{2}H NMR studies are complementary to ^{13}C NMR and similar information can be obtained in both cases. In addition to providing new structural knowledge, ^{2}H NMR studies of lipid bilayers may also prove useful in interpreting the more complex proton (^{1}H) NMR spectra and relaxation properties of the membraneous constituents of cells and tissues. Since the quadrupolar Hamil-

† Alfred P. Sloan Research Fellow.

(1) Presented at 28th Annual Biophysical Society Meeting, San Antonio, Texas, February 1984 (Williams, G. D.; Beach, J. M.; Lustig, S. R.; Dodd, S. W.; Salmon, A.; Brown, M. F. *Biophys. J.* **1984**, *45*, 169a) and the 29th Annual Biophysical Society Meeting, Baltimore, Maryland, February 1985 (Beach, J. M.; Brown, M. F.; Dodd, S. W.; Salmon, A.; Williams, G. D. *Biophys. J.* **1985**, *47*, 247a).

(2) Seelig, J. *Q. Rev. Biophys.* **1977**, *10*, 353-418.
(3) Seelig, J.; Seelig, A. *Q. Rev. Biophys.* **1980**, *13*, 19-61.
(4) Davis, J. H. *Biochim. Biophys. Acta* **1983**, *737*, 117-171.
(5) Smith, R. L.; Oldfield, E. *Science* **1984**, *225*, 280-288.

0002-7863/85/1507-6868$01.50/0